Eur. Phys. J. D **43**, 267–270 (2007)
DOI: 10.1140/epjd/e2007-00065-1

THE EUROPEAN PHYSICAL JOURNAL D

Electronic properties of arrayed K clusters in zeolite LTA with Si/Al = 1.5

T. Kodaira[1,2,a], S. Inoue[1], and Y. Murakami[1]

[1] National Institute of Advanced Industrial Science and Technology (AIST), 1-1-1 Higashi, Tsukuba, Ibaraki 305-8565, Japan
[2] PRESTO, Japan Science and Technology Corporation (JST), Japan

Received 24 July 2006
Published online 24 May 2007 –

Abstract. Arrayed cationic K clusters including one 4*s*-electron in each cluster, i.e., K_{m+1}^{m+}, were incorporated into α-cages of zeolite LTA with Si/Al = 1.5. Although no magnetic phase transition was observed regarding the temperature (T) dependence of magnetic susceptibilities originating from the 4*s*-electron spins ($\chi_{\rm spin}$) between 2 and 300 K, the $\chi_{\rm spin} - T$ curve could be fitted by the sum of magnetic susceptibilities based on the Curie-Weiss law and Pauli paramagnetism. A possible explanation of this behavior is the existence of a narrow energy band formed out of 1*s*-cluster orbitals of arrayed K clusters, and the existence of a finite density of state at the Fermi energy.

PACS. 82.75.Vx Clusters in zeolites – 73.22-.f Electronic structure of nanoscale materials: clusters, nanoparticles, nanotubes, and nanocrystals

1 Introduction

Since the superconductivity of K atom-doped C_{60} crystals [1] was first reported, electronic properties of arrayed and interacting clusters have for the last decade been the subject of much interest [2,3]. Si clathrate, whose electronic structure is based on a Si_{20} unit [4], also exhibits superconductivity [2]. In regard to the macroscopic physical properties of arrayed cluster systems, i.e., magnetism, electric conductivity and so on, the type of interaction among the clusters and its magnitude play significant roles.

Zeolites, which are microporous crystals, can be a host to stabilize arrayed clusters. Potassium (K) clusters in K-form zeolite LTA ($K_{12}Al_{12}Si_{12}O_{48}$:K-LTA(1)) exhibit ferromagnetism despite their lack of inclusion of magnetic elements [5]. In LTA, α-cages with an inner diameter of ca. 1.1 nm are connected, sharing eight-membered rings (8MR) as shown in Figure 1. These α-cages are arrayed in a simple cubic structure with a lattice constant of 1.2 nm. Because loaded guest 4*s*-electrons are shared with both loaded and host K^+ ions as seen in the figure, K clusters are highly cationic and interact with each other through the 8MR. Further detailed experimental facts have been elucidated: the arrayed K clusters are a Mott insulator [6], the adjacent clusters have an antiferromagnetic interaction [6], and local electron-spins of $S = 1/2$ distributing degenerated 1*p* cluster orbitals in each cluster [7,8] array antiparallelly with a cant [9] leading to spontaneous macroscopic magnetization (spin cant ferromagnetism).

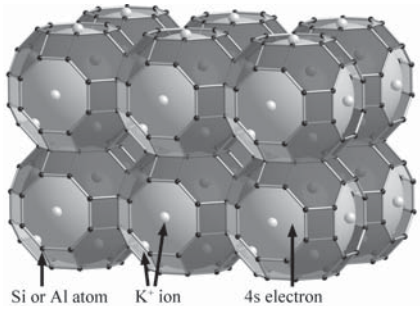

Fig. 1. Arrayed cationic K clusters in α-cages of K-form LTA. O atoms existing between Si or Al atoms in the framework are omitted.

In general, zeolites are non-stoichiometric compounds. A number of years ago, we synthesized K-form zeolite LTAs with various chemical compositions [10]. We could stabilize K clusters in the α-cages of these LTAs [11]. The electronic properties of the clusters should be sensitive to the composition of LTA because, as mentioned, the clusters are cationic. We concluded that K-form LTA with a Si-to-Al atomic ratio of 1.5 (K-LTA(1.5)) provides the largest electron transfer energy between the adjacent clusters [12]. Cluster orbitals of 1*s* and 1*p* for the loaded 4*s*-electrons are formed in the K clusters in K-LTA(1.5) as well as those in K-LTA(1) [13]. In this article, we report

[a] e-mail: kodaira-t@aist.go.jp

the magnetic property of K clusters in K-LTA(1.5) having one 4*s*-electron in each cluster.

2 Experimental

The actual chemical composition of K-LTA(1.5) was $K_{9.1}H_{0.4}Al_{9.5}Si_{14.5}O_{48}$. By adsorbing K atoms into dehydrated K-LTA(1.5) through the vapor phase, K clusters were incorporated into the α-cages [10,11]. The loading density of K atoms per α-cage was 1 ± 0.1. For reference, a sample with a loading density of ca. 0.01 atom per α-cage was prepared. These two samples are described as $K_{1.0}$/K-LTA(1.5) and $K_{0.01}$/K-LTA(1.5), respectively.

The DC magnetic susceptibilities (χ_{DC}) of $K_{1.0}$/K-LTA(1.5) were measured using a SQUID magnetometer. An external magnetic field of 1×10^4 Oe was supplied during the measurement of the temperature dependence. In order to obtain an electron-spin susceptibility (χ_{spin}), we have to subtract diamagnetic susceptibility (χ_{dia}) originating from a quartz sample glass tube, the LTA framework, and K^+ ions from χ_{DC} because of a relation of $\chi_{DC} = \chi_{spin} + \chi_{dia}$.

We measured supplementarily the X-band ESR spectra to obtain χ_{spin}. The obtained relative intensities of the ESR spectra were calibrated by measuring a paramagnetic $CuSO_4{\cdot}5H_2O$ standard sample. The temperature dependence of microwave absorption intensities is proportional to that of χ_{spin}. By subtracting temperature-independent χ_{dia} from χ_{DC}, we could obtain χ_{spin}.

Diffuse reflection spectra were measured and converted into absorption spectra using the Kubelka-Munk function, $A_{KM} = \alpha/S = (1-r)^2/2r$, where α is the absorption coefficient, S the scattering coefficient, and r the diffuse reflectivity. S roughly corresponds to the reciprocal of an average crystal size of the powder. K-LTA(1.5) powder crystals have a cubic shape with an average size of ca. 1 μm.

3 Results and discussion

3.1 Optical properties

Absorption spectrum of $K_{1.0}$/K-LTA(1.5) shown in Figure 2 shows strong absorption around 1.0 eV. Minor absorption can be observed between 2.0 and 5.0 eV. Because the absorption of $K_{0.01}$/K-LTA(1.5) at ca. 1.0 eV was assigned to an optical transition between 1*s* and 1*p* cluster orbitals of cationic K clusters in the α-cage [11], we can conclude that a cationic K cluster also exists in each α-cage at $K_{1.0}$/K-LTA(1.5).

The 4*s*-electrons of loaded K atoms are distributed in the 1*s* cluster orbital of the K clusters. The possibility that two 4*s*-electrons occupy the 1*s* orbital and form a closed structure (a spin singlet state) is very low, as will be explained in Section 3.3. Therefore, the local structure of the K clusters is K_{m+1}^{m+}. Since all the K^+ sites illustrated in Figure 1 are not completely occupied, m may have some

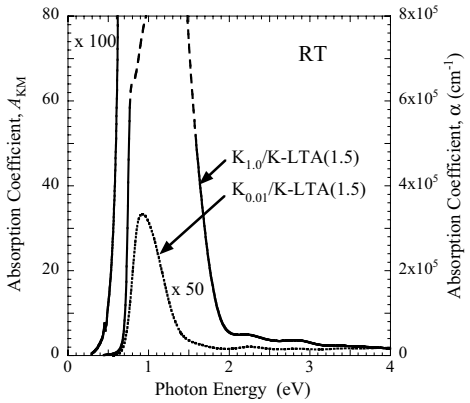

Fig. 2. Absorption spectra of $K_{1.0}$/K-LTA(1.5) (solid curve) and $K_{0.01}$/K-LTA(1.5) (dotted curve) at RT. The broken line region is not transformed correctly into the absorption spectrum. The left vertical axis plotted in the absorption coefficient, α, is for reference.

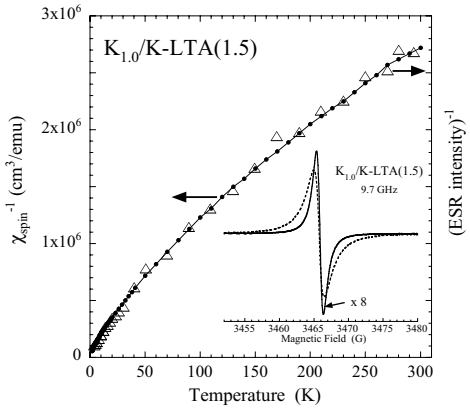

Fig. 3. Temperature dependence of χ_{spin}^{-1}. Closed circles are obtained from χ_{DC} data, and open triangles indicate ESR data. The inset is the representative ESR spectra at 295 (solid curve) and 5 K (broken curve) for reference.

degree of distribution over different cages. The lower energy side (0.3–0.6 eV) of the $K_{1.0}$/K-LTA(1.5) spectrum is magnified 100 times. This area is discussed in Section 3.3.

3.2 Magnetic properties

The dependence of $1/\chi_{spin}$ on temperature (T) is plotted in Figure 3. χ_{spin} has an order of 10^{-6} emu/cm^3 and neither a peak nor a cusp can be observed, even if the sample temperature is lowered to 2 K. This indicates that the sample is basically paramagnetic in a whole measured temperature region. As clearly seen, however, we cannot fit the data by a linear function of the Curie law. This indicates that the K clusters are not completely isolated from each other but have finite interaction.

We fit the $1/\chi_{spin} - T$ plot in Figure 3 using a sum of susceptibilities based on the Curie-Weiss law and Pauli paramagnetism, which are the models for completely localized electron-spins and for free electrons, respectively,

$$\chi_{spin}(T) = C/(T - T_W) + \chi_{Pauli}, \quad (1)$$

where T_W is the Weiss temperature and χ_{Pauli} is the Pauli magnetic susceptibility. C is the Curie constant described as $C = NJ(J+1)g^2\mu_B^2/3k_B$, where N is a density of the electron-spins, $\hbar J$ is the total angular momentum, g is the g-factor, μ_B is the Bohr magneton, and k_B is the Boltzmann constant. The $1/\chi_{spin} - T$ plot in Figure 3 could be fitted with parameters of $T_W = -3.7$ K, $\chi_{Pauli} = 1.6\times10^{-7}$ emu/cm^3, and $C = 6.7\times10^{-5}$ emu K/cm^3. If all the α-cages are occupied by K clusters with an electron spin of $S = 1/2$, the Curie constant is estimated as 3.5×10^{-4} emu K/cm^3. This indicates that ca. 20% of the α-cages are occupied by K clusters in which a 4s-electron is distributed in a 1s cluster orbital. As mentioned in Section 3.1, however, all α-cages are occupied by the K clusters.

The magnetic susceptibility of bulk K metal is insensitive to temperature and has a value of 6×10^{-7} emu/cm^3 (Pauli magnetism). Considering this bulk value, our obtained χ_{Pauli} value seems to be physical, because if the electron density becomes lower, the value of the χ_{Pauli} usually becomes smaller.

In the case of utilizing K-LTA(1) which exhibits ferromagnetism at high K atom loading, the magnetic properties of K clusters with one 4s-electron in each cluster obey the Curie-Weiss law [7,14]. This sample exhibits no ferromagnetism with $T_W \sim 0$ K and $C = 5\times10^{-5}$ emu K/cm^3. Comparing the Weiss temperatures of K clusters in two different hosts, we suspect larger antiferromagnetic exchange interaction between adjacent clusters on $K_{1.0}$/K-LTA(1.5). The shallow potential might cause a spill-out of the 4s-electron wavefunction from the α-cage which induce the finite overlapping of the electron wavefunction between the neighboring cages.

The magnetization curves of $K_{1.0}$/K-LTA(1.5) are also measured at 1.9 and 5.0 K by applying an external magnetic field of $0 \le H \le 7\times10^4$ Oe as drawn in Figure 4 whose horizontal axis is normalized by temperature. For reference, the magnetization curve of an isolated electron spin of $S = 1/2$ in each α-cage is calculated based on the Langevin function, $M = N\mu_B \tanh(\mu_B H/k_B T)$. The experimental magnetization curve at 1.9 K does not saturate even if an external magnetic field of 7×10^4 Oe is applied. Furthermore, the magnetization of $K_{1.0}$/K-LTA(1.5) is about ten times smaller than that of the calculation. Considering all these experimental facts, in the following we discuss the electronic structure of $K_{1.0}$/K-LTA(1.5).

3.3 Electronic structure of $K_{1.0}$/K-LTA(1.5)

As described in Section 3.1, the loaded 4s-electrons into K-LTA(1.5) are distributed in the 1s-cluster orbitals of the K clusters in the α-cage, because only the absorption band for the 1s–1p photo excitation at 1.0 eV are observed. This indicates that 4s-electrons are not directly doped into the LTA framework. The possibility that two 4s-electrons occupy the 1s cluster orbital can be denied, because the observation of the motional narrowing on the ESR spectrum of $K_{0.01}$/K-LTA(1.5) indicates that 4s-electrons are sufficiently mobile to reduce the repulsive energy between

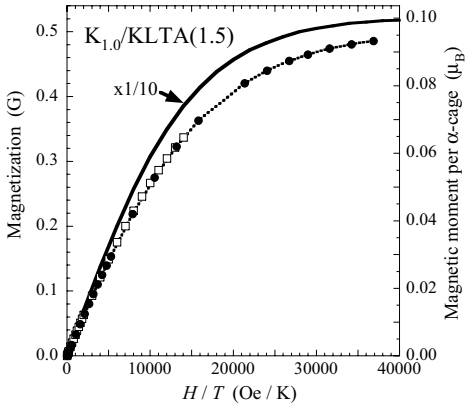

Fig. 4. Magnetization curves at 1.9 (closed circles) and 5.0 (open squares) K. The thick solid curve is the Langevin function with a spin of $S = 1/2$ in each α-cage.

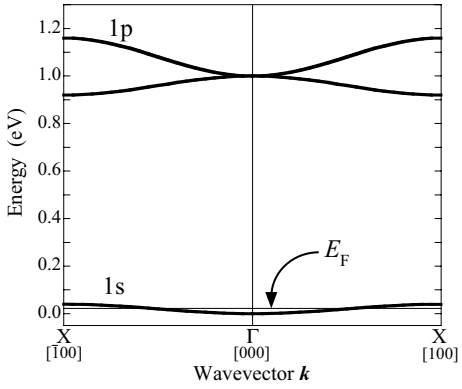

Fig. 5. Schematic drawing of 1s and 1p energy bands for arrayed K clusters in K-LTA(1.5). The 1s band is half filled by the 4s-electrons. E_F is the Fermi energy.

the 4s-electrons [12]. Therefore, arrayed K_{m+1}^{m+} clusters are basically the origin of the optical and magnetic behaviors.

We have adopted a model in Section 3.2 in which two kinds of opposite electronic characters, i.e., localized electron spin and free electron gas, contribute to the magnetic properties to analyze the $1/\chi_{spin} - T$ plot shown in Figure 3. However, only the 4s-electrons, which occupy the 1s cluster orbitals of the K clusters in the α-cages, contribute to the magnetic properties. Therefore, the actual electronic property of the 4s-electrons might exist at an intermediate position between these two opposite models.

If the loaded 4s-electrons distribute periodic potential based on the arrayed K clusters, the energy bands based on the 1s and 1p cluster orbitals might be formed ideally as illustrated in Figure 5. As discussed, the optical transition can be well explained by a model in which the 4s-electron is confined to a potential whose size is defined by the size of the α-cage. Therefore, the energy width of the half-filled 1s band might be very small. On the calculation of the energy bands of K-LTA(1) including the arrayed K clusters with one 4s-electron in each cluster, the bands obtained in a tight-binding approximation using the 1s and 1p cluster orbitals coincide well to the first-principle band calculation [15]. The valence band based on the 1s

orbital had a width of ca. 10 meV in this calculation. In the present case, although the chemical composition of the host K-LTA is slightly different, the energy band regime shown in Figure 5 seems to be basically adequate. The $1p$ band at the Γ-point is triply degenerated in Figure 5, but we presently have no information indicating that the local structure of the K clusters has a cubic symmetry. Furthermore, the actual potential is not completely periodic because the number of K^+ ions, m, is not the same for all α-cages as explained. But we cannot estimate the quantitative influence of the potential fluctuation for the energy band model.

Considering this band effect, we can understand the behavior of the $1/\chi_{\rm spin} - T$ plot fitted by equation (1). A finite density of state exists at the Fermi energy, $E_{\rm F}$, of the narrow $1s$ band. Namely, the half-filled $1s$-band indicates that the arrayed K clusters act as a metal. This is the reason that the magnetization curve shows great difficulty in saturating the magnetization. Evidence of a metallic state should be also observed in the optical spectrum. For example, if the $4s$-electrons loaded into K-LTA(1.5) act as free electrons, the bulk plasmon energy $\hbar\omega_{\rm p}$ can be estimated as 0.7 eV using the equation

$$\omega_{\rm p} = \sqrt{4\pi n e^2/m_e}, \qquad (2)$$

where n is the density of conduction electrons and m_e is the mass of an electron. As plotted as the magnified area in Figure 2, however, no Drude term whose energetic position corresponds to the bulk plasmon energy can be observed. Because of the narrow $1s$-band, the effective mass of the electron in the $1s$ band is heavy. If m_e in equation (2) is substituted by an effective mass m_e^*, m_e^* may be larger than $20m_{\rm e}$ which gives $\hbar\omega_{\rm p} < 0.2$ eV. Or, because the band regime includes only the Pauli exclusion principle, the finite interaction between the clusters might induce a low density of state at the Fermi level by the electron correlation. Any way, we could not detect the metallic state in the present optical measurement.

In this discussion, we treated the LTA framework to act merely as a container of the arrayed K clusters. However, the large transfer energy between the adjacent K clusters is produced by the shallow potential in the K cluster for the $4s$-electrons. This indicates that the electron wave function can be spilled out from the K cluster and may interact with the LTA framework [16]. In future, in order to arrive at a definitive conclusion, we have to investigate the electronic structures in detail based on the experimental data of the arrayed K clusters in K-LTA(1.5) with systematic control of the K atom loading density.

Finally, we briefly compare our sample with electrosodalite which is also a cluster-arrayed system. β-cages, whose inner diameter is ca. 0.7 nm, are arrayed in a body centered cubic structure in sodalite. Sodium and potassium electro sodalite (SOD) exhibit a Mott insulator type antiferromagnetism whose Néel temperatures are 50.3±0.2 and 71±2 K, respectively [17,18]. By applying high static pressure to these compounds, both Néel and Weiss temperatures decrease because of increased interaction between the clusters [19]. Although the arrangement of the clusters in LTA is different from SOD, the increased interaction may weaken the thermal stability on the macroscopic ordering of the unpaired electrons.

4 Summary

Arrayed K clusters with one $4s$-electron in each cluster were incorporated into K-LTA(1.5). The $4s$-electron distributes the $1s$ cluster orbital. The $1/\chi_{\rm spin} - T$ plot can be fitted by a sum of the magnetic susceptibilities obeying the Curie-Weiss law and Pauli paramagnetism. This indicates that a finite interaction between the adjacent K clusters. There may be a finite density of state at the Fermi energy of the narrow $1s$ band.

T.K. thanks Dr. Kawaguchi for using his SQUID magnetometer.

References

1. R.C. Haddon, A.F. Hebard, M.J. Rosseinsky, D.W. Murphy, S.J. Duclos, K.B. Lyons, B. Miller, J.M. Rosamilia, R.M. Fleming, A.R. Kortan, S.H. Glarum, A.V. Makhija, A.J. Muller, R.H. Eick, S.M. Zahurak, R. Tycko, G. Dabbagh, F.A. Thiel, Nature **350**, 320 (1991)
2. H. Kawaji, H. Horie, S. Yamanaka, M. Ishikawa, Phys. Rev. Lett. **74**, 1427 (1995)
3. F. Liu, M. Mostoller, T. Kaplan, S.N. Khanna, P. Jena, Chem. Phys. Lett. **248**, 213 (1996)
4. S. Saitoh, A. Oshiyama, Phys. Rev. B **51**, 2628 (1995)
5. Y. Nozue, T. Kodaira, T. Goto, Phys. Rev. Lett. **68**, 3789 (1992)
6. T. Nakano, Y. Ikemoto, Y. Nozue, Eur. Phys. J. D **9**, 505 (1999)
7. T. Nakano, Y. Ikemoto, Y. Nozue, Phys. B **281–282**, 688 (2000)
8. T. Nakano, Y. Ikemoto, Y. Nozue, J. Phys. Soc. Jpn **71**, (2002) Suppl. pp. 199
9. T. Nakano, D. Kiniwa, Y. Ikemoto, Y. Nozue, J. Mag. Mag. Mater. **272–276**, 114 (2004)
10. T. Ikeda, T. Kodaira, T. Oh, A. Nisawa, Microporous Mesoporous Mater. **57**, 249 (2003)
11. T. Oh, J.-S. Yu, T. Ikeda, T. Kodaira, Solid State Commun. **123**, 387 (2002)
12. T. Kodaira, Y. Murakami, submitted
13. T. Kodaira, Y. Murakami, S. Inoue, Phys. B **359–361**, 1445 (2005)
14. T. Nakano, Y. Ikemoto, Y. Nozue, J. Mag. Mag. Mater. **226–230**, 238 (2001)
15. R. Arita, T. Miyake, T. Kotani, M. van Schilfgaarde, T. Oka, K. Kuroki, Y. Nozue, H. Aoki, Phys. Rev. B **69**, 195106 (2004)
16. M. Igarashi, T. Kodaira, T. Shimizu, A. Goto, K. Hashi, J. Phys. Chem. Solids **67**, 1063 (2006)
17. R. Scheuermann, E. Roduner, G. Engelhart, H.-H. Klauss, D. Herlach, Phys. Rev. B **66**, 144429 (2002)
18. L. Damjanovic, G.D. Stucky, V.I. Srdanov, J. Serb. Chem. Soc. **65**, 311 (2000)
19. K. Mizoguchi, T. Yamabe, H. Sakamoto, Lj. Damjanovic, V.I. Srdanov, Synth. Metals **137**, 909 (2003)